

# UC Santa Barbara

## UC Santa Barbara Previously Published Works

### Title

Compact 160-Gb/s add-drop multiplexer with a 40-Gb/s base rate using electroabsorption modulators

### Permalink

<https://escholarship.org/uc/item/1n33f7zx>

### Journal

IEEE Photonics Technology Letters, 16(6)

### ISSN

1041-1135

### Authors

Chou, H F  
Bowers, John E

### Publication Date

2004-06-01

Peer reviewed

# Compact 160-Gb/s Add-Drop Multiplexer With a 40-Gb/s Base Rate Using Electroabsorption Modulators

Hsu-Feng Chou, John E. Bowers, *Fellow, IEEE*, and Daniel J. Blumenthal, *Fellow, IEEE*

**Abstract**—We report on the first 40-Gb/s-based 160-Gb/s add-drop multiplexer (ADM) using a pair of standing-wave enhanced electroabsorption modulator (EAM). Direct time-domain switching is performed without interferometers or optical control pulses as required by previously reported approaches, which indicates great advantages in compactness for the EAM-based ADM. Also, a 40-Gb/s base rate is attractive in realizing a more efficient 160-Gb/s system. Error-free operation for all channels is obtained with an average power penalty as low as 1 dB.

**Index Terms**—Add-drop multiplexing, electroabsorption, optical time-division multiplexing (OTDM), standing-wave device, traveling-wave device.

## I. INTRODUCTION

**T**IME-DOMAIN add-drop multiplexing (ADM) is an essential function in an optical time-division multiplexed (OTDM) network. Two operations are performed in an ADM node: 1) a base-rate channel is extracted from the high-speed line signal (drop function); 2) the time slot of the dropped channel is cleared and a new channel is inserted while the through channels remain undisturbed (add function). These operations require two complementary switching windows with well-defined shapes, which becomes more challenging as the bit rate increases. ADMs with a 160-Gb/s line rate were not reported until recently [1], [2]. These demonstrations utilized gain-transparent operation of a semiconductor optical amplifier (SOA) to reduce pattern effects and noise in conventional SOA-based interferometric switches [3]. However, these setups are complex and a high-quality optical control pulse is required at the base rate. An electroabsorption modulator (EAM) is another choice for high-speed switching, and a 40-Gb/s ADM was demonstrated with a 10-Gb/s base rate [4]. The advantages of using EAMs include the following: 1) the switching window is generated without an interferometer; 2) only an electrical control signal is required. Consequently, EAMs are promising for more compact ADM. Nevertheless, the width of the switching window needed to be shortened in order to scale the operation to 160 Gb/s.

In this letter, we demonstrate the first 160-Gb/s ADM with a 40-Gb/s base rate using EAMs. The switching window of

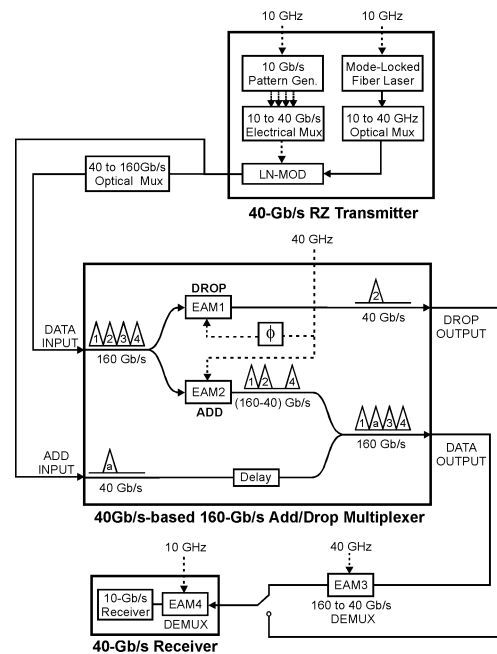


Fig. 1. Schematic setup of the 40-Gb/s-based ADM using EAMs. Solid line: optical link. Dotted line: electrical link.

the EAM is shortened by increasing the driving frequency to 40 GHz and also by using a standing-wave enhanced design [5]. Even though mixing microwave harmonics can also shorten the switching window of the EAM with a 10-Gb/s base rate [6], upgrading the base rate to 40 Gb/s leads to a more compact and efficient OTDM system. It is worth nothing that while a 40-Gb/s base rate favors the EAM for 160-Gb/s operation, it is more challenging for SOA-based switches due the limitation of carrier lifetime [7].

## II. EXPERIMENT AND RESULTS

The configuration of the 40-Gb/s-based ADM is shown schematically in Fig. 1. Two EAMs are used to implement the drop function (EAM1) and the add function (EAM2) individually. A new channel can be added with the through channels passively with a coupler and a delay line. The only differences between the two EAMs are the bias voltage and the phase of the 40-GHz driving signal, which implies that single-chip integration is possible. The EAM used in this work has traveling-wave electrodes [coplanar waveguide (CPW)] designed to overcome the resistance-capacitance time limitation [8]. The device is

Manuscript received January 27, 2004; revised February 18, 2004. This work was supported by The Defense Advanced Research Project Agency (DARPA).

The authors are with the Department of Electrical and Computer Engineering, University of California, Santa Barbara, Santa Barbara, CA 93106-9560 USA (e-mail: hubert@ece.ucsb.edu).

Digital Object Identifier 10.1109/LPT.2004.827118

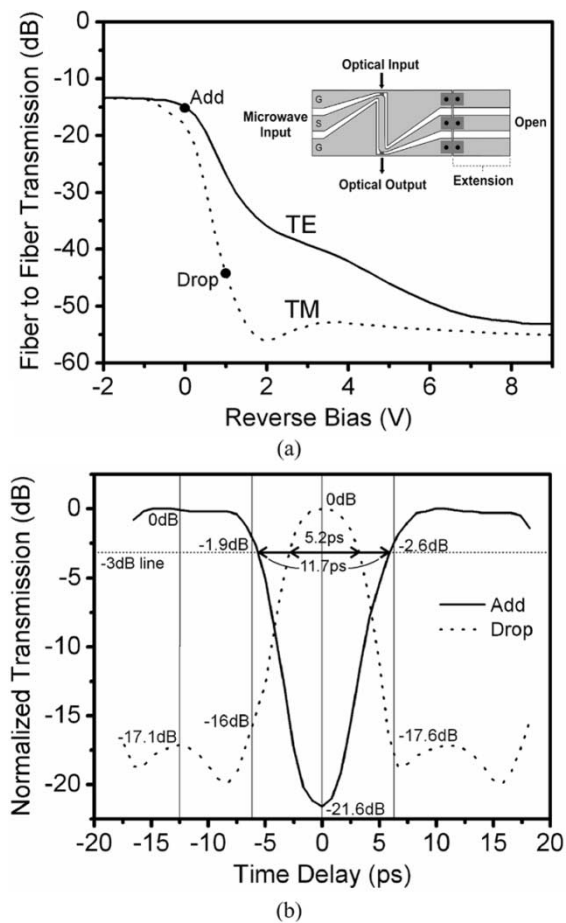


Fig. 2. (a) Static fiber-to-fiber transmission of the EAM for TE and TM polarizations at 1557.5 nm. The solid circles are the bias points for respective operations. Insert: Layout of the standing-wave enhanced EAM. (b) Dynamic transmission at 40 GHz measured by scanning a 1.5-ps pulse train. The vertical lines are spaced by 6.25 ps.

1000  $\mu\text{m}$  long and 330  $\mu\text{m}$  wide. With a 35- $\Omega$  termination, the bandwidth is  $>20$  GHz. The static fiber-to-fiber transmissions for the transverse-electric (TE) and transverse-magnetic (TM) polarizations at 1557.5 nm are shown in Fig. 2(a), together with the layout of the standing-wave enhanced mode. To enhance the electrooptical response at 40 GHz, a microwave standing-wave pattern is formed along the CPW line by adopting an open termination [5]. The spatial phase is adjusted with a 500- $\mu\text{m}$  extension CPW line so that the microwave amplitude and distribution can be optimized in the active waveguide. TE polarization is chosen for the add function and TM for the drop function, which minimizes the gating windows for the respective operations. The polarization dependence can be reduced by properly compensating the strain in the quantum wells [9]. The bias voltage is 0 V for the add function and  $-1$  V for the drop function. The EAM is driven by a 6  $V_{p-p}$  40-GHz sinusoidal microwave. By scanning a 1.5-ps 10-GHz optical pulse train through the EAM, the gating windows are obtained as shown in Fig. 2(b), which represents the closest estimation of actual performance since the pulse source is the same as that used in the transmitter. The traces are shifted by 180° in phase (12.5 ps) relative to each other for clearer illustration. Due to the high modulation efficiency of the EAM, the switching window can be changed for the opposite operation by adjusting

only 1 V in bias voltage. As shown in Fig. 2(b), the 3-dB width of the gating window is 11.7 ps for the add function and 5.2 ps for the drop function. If the polarizations are switched, the gating windows will be broadened to 13.3 and 6.8 ps, respectively. The suppression of adjacent channels is over 16 dB in the drop function and the clearing of the targeted time slot is over 21 dB in the add function. However, there can be a variation of 1.9–2.6 dB in power among the through channels in the add function. This is not a fundamental limitation of EAM-based ADM and can be reduced by moving the bias point upwards along the transmission curve in Fig. 2(a). However, the extinction ratio may be reduced. In that case, the effective driving voltage must be increased by either a higher driving power or an impedance matching network to obtain the required extinction ratio.

As shown in Fig. 1, a 40-Gb/s nonreturn-to-zero electrical signal is generated from four 10-Gb/s  $2^7 - 1$  pseudorandom-binary-sequence (PRBS) tributaries using an electrical multiplexer. The PRBS word length is limited by the electrical multiplexer. This 40-Gb/s signal drives a LiNbO<sub>3</sub> modulator to encode a 40-GHz optical pulse train, which is passively multiplexed from a 10-GHz 1.5-ps pulse train generated by a mode-locked fiber laser centered at 1557.5 nm. The output 40-Gb/s RZ signal is split into two parts. One is further multiplexed to 160 Gb/s with a single polarization and the other is used as the added channel. The PRBS character is not truly preserved at 160 Gb/s but several meters of delay are used to decorrelate the tributaries. The phase delay  $\phi$  of the 40-GHz driving signal to EAM1 is set to 180° in order to implement ADM on the same channel. An advantage of the presented approach is the flexibility of simultaneous ADM on different channels by changing the value of  $\phi$ . On the receiver side, EAM3 is used to demultiplex 160-Gb/s signals back to 40 Gb/s. Note that the operations of EAM3 in the receiver (demultiplexing) and EAM1 in the ADM (drop function) are actually the same. The 40-Gb/s receiver is composed of an optical 40- to 10-Gb/s demultiplexer (EAM4) and a 10-Gb/s electrical receiver. Even though the ADM is working with a 40-Gb/s base rate, bit-error rate (BER) is measured at 10 Gb/s for all 16 channels. BER measurement can be implemented at 40 Gb/s when a 40-Gb/s BER tester is available. The input average power levels to EAM1, EAM2, and EAM3 in the experiment are approximately  $-1$  dBm per 40-Gb/s channel, corresponding to a peak power of 14.2 dBm.

The eye diagrams of the 160-Gb/s signals cannot be fully resolved by using a 50-GHz electrical sampling scope with a 40-GHz photodetector. Instead, the 160-Gb/s signals are sampled after the 160- to 40-Gb/s demultiplexer (EAM3), which extracts the four 40-Gb/s channels individually. Fig. 3(a) shows the eye diagrams of the four channels in the back-to-back (BtB) 160-Gb/s signal. The bumps on the bottom of the eyes are caused by the response of the photodetector. After EAM2, a 40-Gb/s channel (ch. 2) is cleared, as shown in Fig. 3(b). The eye amplitude of ch. 4 is about 2 dB higher than the other two through channels, in agreement with the pulse scanning results in Fig. 2(b). A new 40-Gb/s channel is then added to the cleared time slot with the same polarization as the through channels and Fig. 3(c) shows no observable sign of interference.

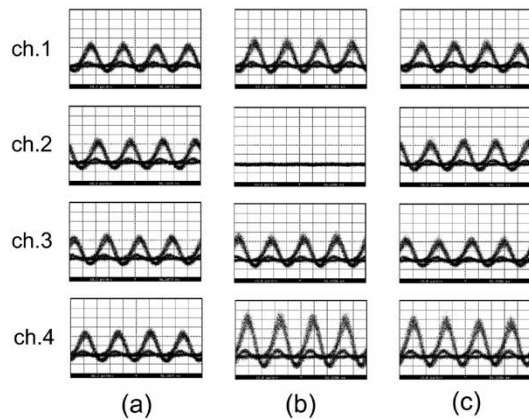


Fig. 3. 40-Gb/s eye diagrams of the four channels in the 160-Gb/s signal (a) back to back, (b) after ch. 2 is dropped, and (c) after a new 40-Gb/s channel is added.

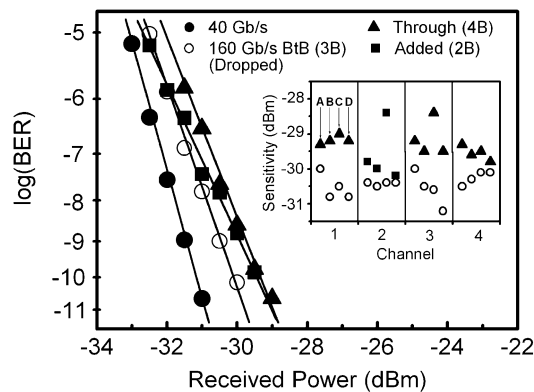


Fig. 4. BER curves measured at 10 Gb/s. The insert shows the receiver sensitivities of the four 10-Gb/s tributaries in each 40-Gb/s channel.

Fig. 4 shows the results of BER measurements. The received power is measured at the input of the 10-Gb/s receiver. Power penalty and receiver sensitivity are measured at a BER of  $1e-9$ . The 40-Gb/s line is obtained by sending a 40-Gb/s signal to the 160-Gb/s receiver (EAM3 plus the 40-Gb/s receiver). There is a 1-dB power penalty when the input is changed to the 160-Gb/s BtB signal. The penalty mainly comes from the finite suppression ratio of the 160- to 40-Gb/s demultiplexer. Note that the 160-Gb/s BtB line also represents the BER result for the dropped channel since the operation of EAM1 and EAM3 are identical as mentioned above. After ADM, the averaged power penalty for the four 40-Gb/s channels (ch. 1–4) are 1.3, 0.8, 1.4, and 0.7 dB, respectively, which results in an overall

power penalty of 1 dB. A low power penalty of 0.8 dB for the added channel (ch. 2) indicates that the clearing of the time slot in the add function is successful and the interference with the residue of the dropped channel is negligible. The 2-dB variation in power among the through channels (ch. 1, 3, and 4) only results in a 0.6 – 0.7-dB difference in power penalty, which is believed to be a consequence of the varied signal-to-noise ratio due to the power variation.

### III. CONCLUSION

By using standing-wave enhanced EAMs, 160-Gb/s ADM with a 40-Gb/s base rate has been demonstrated. The averaged power penalty is as low as 1 dB. The setup is simpler than the previously reported approaches, where interferometers and optical control pulses are required. Together with a high 40-Gb/s base rate, this work shows that compact and efficient ADMs can be realized with EAMs.

### REFERENCES

- [1] C. Schubert, C. Schmidt, S. Ferber, R. Ludwig, and H. G. Weber, "Error-free all optical add-drop multiplexing at 160 Gbit/s," *Electron. Lett.*, vol. 39, no. 14, pp. 1074–1076, July 2003.
- [2] J. P. Turkiewicz, H. Rohde, W. Schairer, G. Lehmann, E. Tangdiongga, G. D. Khoe, and H. de Waardt, "All-optical OTDM add-drop node at  $16 \times 10$  Gbit/s in between two fiber links of 150 km," in *Proc. 29th Eur. Conf. Optical Communication*, vol. 6, Sept. 2003, Postdeadline Paper Th4.4.5, pp. 84–85.
- [3] S. Diez, R. Ludwig, and H. G. Weber, "Gain-transparent SOA-Switch for high-bitrate OTDM add/drop multiplexing," *IEEE Photon. Technol. Lett.*, vol. 11, pp. 60–62, Jan. 1999.
- [4] I. D. Phillips, A. Gloag, D. G. Moodie, N. J. Doran, I. Bennion, and A. D. Ellis, "Drop and insert multiplexing with simultaneous clock recovery using an electroabsorption modulator," *IEEE Photon. Technol. Lett.*, vol. 10, pp. 291–293, Feb. 1998.
- [5] H.-F. Chou, Y.-J. Chiu, and J. E. Bowers, "Standing-wave enhanced electroabsorption modulator for 40-GHz optical pulse generation," *IEEE Photon. Technol. Lett.*, vol. 15, pp. 215–217, Feb. 2003.
- [6] H.-F. Chou, Y.-J. Chiu, W. Wang, J. E. Bowers, and D. J. Blumenthal, "Compact 160-Gb/s demultiplexer using a single-stage electrically gated electroabsorption modulator," *IEEE Photon. Technol. Lett.*, vol. 15, pp. 1458–1460, Oct. 2003.
- [7] G. Toptchiyski, S. Randel, K. Petermann, C. Schubert, J. Berger, and H. G. Weber, "Characterization of switching windows of an 160-Gb/s all-optical demultiplexer with data base rates of 10 and 40 Gb/s," *IEEE Photon. Technol. Lett.*, vol. 14, pp. 534–536, Apr. 2002.
- [8] Y.-J. Chiu, H.-F. Chou, V. Kaman, P. Abraham, and J. E. Bowers, "High extinction ration and saturation power traveling-wave electroabsorption modulator," *IEEE Photon. Technol. Lett.*, vol. 14, pp. 792–794, June 2002.
- [9] S. Z. Zhang, Y.-J. Chiu, P. Abraham, and J. E. Bowers, "25-GHz polarization-insensitive electroabsorption modulators with traveling-wave electrodes," *IEEE Photon. Technol. Lett.*, vol. 11, pp. 191–193, Feb. 1999.